



Published in final edited form as:

Oncogene. 2016 May 5; 35(18): 2390–2397. doi:10.1038/onc.2015.302.

Sustained adrenergic signaling leads to increased metastasis in ovarian cancer *via* increased PGE2 synthesis

Archana S. Nagaraja¹, Piotr L. Dorniak¹, Nouara C. Sadaoui¹, Yu Kang¹, Tan Lin², Guillermo Armaiz-Pena¹, Sherry Y. Wu¹, Rajesha Rupaimoole¹, Julie K. Allen¹, Kshipra M. Gharpure¹, Sunila Pradeep¹, Behrouz Zand¹, Rebecca A. Previs¹, Jean M. Hansen¹, Cristina Ivan³, Cristian Rodriguez-Aguayo³, Peiyang Yang², Gabriel Lopez-Berestein³, Susan K. Lutgendorf⁵, Steve W. Cole⁶, and Anil K. Sood^{1,3,4}

¹Department of Gynecologic Oncology and Reproductive Medicine, The University of Texas MD Anderson Cancer Center, Houston, TX 77030

²Department of General Oncology, The University of Texas MD Anderson Cancer Center, Houston, TX 77030

³Center for RNAi and Non-Coding RNA, The University of Texas MD Anderson Cancer Center, Houston, TX 77030

⁴Department of Cancer Biology, The University of Texas MD Anderson Cancer Center, Houston, TX 77030

⁵Department of Psychology, Obstetrics and Gynecology, and Urology and Holden Comprehensive Cancer Center, University of Iowa, Iowa City, IA 52242

⁶Department of Medicine and Jonsson Comprehensive Cancer Center, University of California, Los Angeles School of Medicine, UCLA Molecular Biology Institute, and Norman Cousins Center, Los Angeles, CA 90095

Abstract

Adrenergic stimulation adversely affects tumor growth and metastasis, but the underlying mechanisms are not well understood. Here, we uncovered a novel mechanism by which catecholamines induce inflammation by increasing prostaglandin E2 (PGE2) levels in ovarian cancer cells. Metabolic changes in tumors isolated from patients with depression and mice subjected to restraint stress showed elevated PGE2 levels. Increased metabolites and PTGS2 and

Users may view, print, copy, and download text and data-mine the content in such documents, for the purposes of academic research, subject always to the full Conditions of use:http://www.nature.com/authors/editorial_policies/license.html#terms

Correspondence and reprint requests: Anil K. Sood, MD, Professor and Vice Chair for Translational Research, Departments of Gynecologic Oncology and Cancer Biology, Unit 1352, The University of Texas MD Anderson Cancer Center, 1515 Holcombe Blvd, Houston, TX 77030, USA; phone: 713-745-5266; fax: 713-792-7586; ; Email: asood@mdanderson.org

Author Contributions

A.N. and A.K.S. conceived the project and designed the experiments. A.N., N.C.S., P.L.D., R.A.P., J.K.A., G.A-P., J.M.H., S.P., S.Y.W., B.Z., and K.M.G. carried out or participated in *in vitro* and *in vivo* experiments. C.R.-A. and G.L.-B. designed and prepared liposomes for *in vivo* studies. A.N. and C.I. designed and performed computational analyses. T.L. and P.Y. performed the Mass-spec analysis. A.N. wrote the manuscript. A.N., P.L.D., S.K.L., S.C. and A.K.S. participated in manuscript preparation. All authors edited and approved the final manuscript.

Conflict of Interest

The authors declare no competing financial interests.

PTGES protein levels were found in Skov3-ip1 and HeyA8 cells treated with norepinephrine, and these changes were shown to be mediated by ADRB2 receptor signaling. Silencing PTGS2 resulted in significantly decreased migration and invasion in ovarian cancer cells in the presence of norepinephrine and decreased tumor burden and metastasis in restraint stress orthotopic models. In human ovarian cancer samples, concurrent increased ADRB2, PTGS2 and PTGES expression was associated with reduced overall and progression-free patient survival. In conclusion, increased adrenergic stimulation results in increased PGE2 synthesis via ADRB2-Nf-kB-PTGS2 axis, which drives tumor growth and metastasis.

Introduction

Recent studies have uncovered a role for neuroendocrine factors in tumor progression. For example, clinical studies and pre-clinical studies have shown that chronic psychological distress (e.g., depression, bereavement) can play a pivotal role in disease progression, recurrence, and response to chemotherapy in breast, ovarian, and other cancers¹⁻⁸. Stress effects are mediated by either the sympathetic nervous system (SNS) or the hypothalamic-pituitary-adrenal axis. Chronic activation of the SNS has profound effects on tissue homeostasis and has been shown to exacerbate inflammatory bowel disease, cardiovascular disease, and diabetes and compromise immune function. Preclinical studies have demonstrated that chronic activation of the SNS, mediated primarily by increased synthesis of norepinephrine (NE) can lead to increased angiogenesis, avoidance of anoikis, and tumor cell invasion in cancer models^{6,9,10}.

NE is a potent pro-inflammatory factor, and sustained inflammation mediated by NE can impair wound healing^{11,12}. However, its role in driving tumor inflammation is not well understood. Under chronic stress conditions, increased intratumoral NE levels have been demonstrated⁶. Moreover, patients with high levels of depression and poor social support also have elevated intratumoral NE⁴. Here, we examined the mechanisms by which adrenergic pathways increase the production of pro-inflammatory metabolites in ovarian tumors and the mechanisms by which these pathways promote tumor metastasis.

Results

Effect of biobehavioral stress on metabolism in high-grade serous ovarian cancer

To identify potential metabolic changes in response to elevated stress levels, we performed a global metabolite analysis on human ovarian cancer samples from patients with known levels of depression as well tumoral NE levels. Patients took a standardized questionnaire (the Center for Epidemiologic Studies Depression Scale [CES-D]) and a cutoff score of 16, which has been associated with clinical depression was selected to classify high and low depressive scores¹³. Unbiased analysis of metabolites stratified on the basis of CES-D scores showed significant differences between those with high and low levels of depression in the enrichment of several metabolites (Supplementary Table 1) involved in inflammation, cell proliferation and signaling, as well as metabolites involved in carbohydrate and mineral metabolism. Of special interest are eicosanoids that play a potent role in mediating tumor inflammation.

In both groups, tumor tissue had increased levels of eicosanoids compared with normal ovarian tissue samples (Figure 1A). Higher eicosanoid levels were observed in samples from patients with high CES-D scores (i.e., scores >16) than in those with low CES-D scores (Figure 1A and 1B). Prostaglandin E2 (PGE2) and 6-keto prostaglandin F1 alpha (PGF2a) metabolites were elevated in tumors from those with high CES-D scores compared with those with low scores (PGE2: 2.38-fold increase, $p < 0.05$; PGF2a: 2.03-fold increase, $p < 0.05$). These metabolites play an important role as mediators of inflammatory processes and are known to play a role in tumor biology.

Similar unbiased metabolite analysis of Skov3-ip1 ovarian tumors from mice showed several elevated metabolites (Supplementary Table 2). Similar to the patient samples, tumors from mice subjected to restraint stress for 10 days also showed enriched PGE2 and PGF2a (PGE2: 1.42-fold increase; PGF2a: 1.2-fold increase; Figure 1C and 1D) compared with tumors from control mice. Additionally, these orthotopic tumor samples were assayed using mass spectrometry, which confirmed that PGE2 and PGF2 α levels were increased in tumor samples from mice subjected to restraint stress and presence of substrate arachidonic acid (AA) (Figure 1E).

Role of NE in driving PGE2 synthesis in tumor cells

PGE2 is known to be produced by a 2-step reaction catalyzed by the inducible genes *PTGS2* and *PTGES* and metabolized by *HPGD* (1,5-hydroxyprostaglandin dehydrogenase). To study the underlying mechanism driving adrenergic-induced PGE2 synthesis, we measured the expression of *PTGS2* and *PTGES* in Skov3-ip1 orthotopic tumors from mice subjected to restraint stress by real time PCR (Figure 2A). We observed a time-dependent increase in expression of both genes after 1, 2, or 3 weeks of daily restraint stress. No changes were observed in the levels of genes *PTGS1* and *PTGES2* after restraint stress (data not shown), indicating that elevated PGE2 levels are a result of increased expression of inducible gene *PTGS2*. *PTGS2* protein expression was substantially higher in tumors from mice exposed to daily restraint stress than in tumors from control mice in both Skov3-ip1 and HeyA8 models (Figure 2B and Supplementary Figure 1A); *PTGS1* levels were not significantly different between stress and non-stress tumor samples (Supplementary Figure 1B).

To validate our findings that elevated signaling was due to adrenergic signaling and not due to intratumoral indirect factors, we treated Skov3-ip1 and HeyA8 cells with NE. In both cell lines, relative to control, cells treated with NE showed elevated gene expression of *PTGS2* and *PTGES* (Skov3-ip1: 1.2-fold increase in *PTGS2* and 2.8-fold increase in *PTGES*; HeyA8: 4-fold increase in *PTGS2* and 28.09-fold increase in *PTGES*; Figure 2C). Treatment of ADRB-negative A2780 cells with NE did not induce altered expression levels of *PTGS2* or *PTGES* (Supplementary Figure 1C). Treatment of Skov3-ip1 cells with NE resulted in increases in *PTGS2* protein levels (Figure 2D). Staining of cells treated with NE also increased the abundance of *PTGES* immune-reactive protein within the nucleus in both cell lines (Figure 2E). Treatment of the cells with cortisol did not alter levels of *PTGS2* or *PTGES* in either Skov3-ip1 or HeyA8 cells (Supplementary Figure 1D), indicating that HPA axis is not a key regulator of PGE2 synthesis.

Effect of silencing *PTGS2* on adrenergic-mediated metastasis

To study the functional implications of elevated PGE₂ signaling, we used siRNA to silence *PTGS2*, which is the rate-limiting step in PGE₂ synthesis (Figure 3A). The human-specific sequence, which silenced *PTGS2*, was selected to study the functional effects of *PTGS2* after adrenergic activation. Silencing *PTGS2* using siRNA significantly decreased PGE₂ levels in the media (Figure 2F). In migration and invasion assays, silencing *PTGS2* completely abrogated the effects of NE in Skov3-ip1 cells (Figure 2G and 2H). To examine the effects of silencing *PTGS2 in vivo*, we injected Skov3-ip1 cells into the ovary of athymic nude mice, and tumor burden, number of tumor nodules, and the metastatic pattern were noted at the end of the experiment. Adrenergic-mediated increases in both tumor growth and tumor nodules were significantly decreased after silencing *PTGS2* (Figure 3A and 3B). Silencing *PTGS2* also abrogated the stress-mediated effects on metastatic spread of disease (Figure 3C). Immunohistochemistry and quantitative reverse-transcription polymerase chain reaction (qRT-PCR) were used to assess silencing of *PTGS2* during the course of the animal study (Figure 3D–3E). H&E sections showed increased infiltration of tumors during stress, which was abrogated when *PTGS2* was silenced (Figure 3F).

Mechanism of *PTGS2* induction after treatment with NE

To further study the underlying mechanisms that lead to increased PGE₂ after adrenergic stimulation, we used specific antagonists or agonists of various beta-adrenergic receptors. Only the ADRB₂-specific agonist terbutaline and the broad ADRB agonist isoproterenol increased levels of *PTGS2* and *PTGES* in Skov3-ip1 cells to levels similar to those induced by NE alone (terbutaline: 1.85-fold increase in *PTGS2* and 9.29-fold increase in *PTGES*; isoproterenol: 1.16-fold increase in *PTGS2* and 9.52-fold increase in *PTGES*; Figure 4A). Treatment with specific agonists did not alter levels of *PTGS1* or *PTGES2* in either cell line (Supplementary Figure 2A). Conversely, in both cell lines, the ADRB₂-specific antagonist butoxamine and broad ADRB antagonist propranolol completely abrogated the effects of NE on *PTGS2* and *PTGES* (Figure 4B).

PGE₂ enzyme-linked immunosorbent assay (ELISA) results showed that treatment of 1 million Skov3-ip1 and HeyA8 cells with NE increased PGE₂ levels in media (38.8 pg PGE₂ in Skov3-ip1 cells and 65.1 pg in HeyA8 cells), and this was abrogated when the cells were pretreated with butoxamine (28 pg in Skov3-ip1 cells and 36.35 pg in HeyA8 cells) or propranolol (33.2 pg in Skov3-ip1 cells and 34.15 pg in HeyA8 cells). Additionally, the broad ADRB agonist isoproterenol and the ADRB₂-specific agonist terbutaline significantly increased PGE₂ levels in media (isoproterenol: 41.8 pg PGE₂ in Skov3-ip1 cells and 70.8 pg PGE₂ in HeyA8 cells; terbutaline: 40 pg PGE₂ in Skov3-ip1 cells and 50.65 pg PGE₂ in HeyA8 cells; Figure 4C).

To study the downstream mechanism of activation, we focused on Nf-κB because promoters of both *PTGS2* and *PTGES* have Nf-κB binding sites (Supplementary Figure 2B)¹⁴. In addition, previous analyses have shown that Nf-κB activity is elevated during adrenergic signaling⁴. Treatment of cells with NE increased levels of both p65 and p50 in nucleus after 2 hours (Supplementary figure 2C). Chromatin immunoprecipitation (ChIP) analysis showed enrichment of Nf-κB binding to the promoter region of *PTGS2* (2.4-fold enrichment) and

PTGES (4.0-fold enrichment) when Skov3-ip1 cells were treated with NE (Figure 4D). In Skov3-ip1 cells, levels of p65 and p50 subunits of Nf-kB in the nucleus increased (1.71-fold increase in p65 and 1.76-fold increase in p50) after treatment with NE (Figure 4E).

Clinical importance of *PTGS2* and *PTGES*

We then used data from The Cancer Genome Atlas project for high-grade serous ovarian cancer to determine whether the genes involved in PGE2 synthesis were important for survival. Using the median expression levels as a cutoff for *ADRB2*, *PTGS2* and *PTGES*, we found that increased expression of these genes was associated with significantly reduced progression-free and overall survival (Figure 5A and 5B). Supportive data *in vivo* shows that blocking adrenergic signaling using propranolol or butoxamine decreased *PTGS2* levels in the tumor (supplementary figure 3A).

Taken together, our results indicate that NE can activate the *ADRB2* receptor and transcriptionally activate *PTGS2* and *PTGES* *via* Nf-kB to produce PGE2 (Figure 5C). Silencing *PTGS2* can abrogate stress-mediated ovarian cancer growth *in vivo*.

Discussion

Tumor-promoting inflammation is an emerging hallmark of cancer, and the role of adrenergic signaling in mediating this inflammation is not fully known. In the current study, we present a novel mechanism of production of pro-inflammatory prostaglandins via the *ADRB2*-Nf-kB-*PTGS2*-PGE2 axis. In Skov3-ip1 and HeyA8 orthotopic models of ovarian cancer, we found that blocking adrenergic signaling with a broad beta-blocker (propranolol) or an *ADRB2*-specific blocker (terbutaline) decreased levels of *PTGS2* in tumor cells. Silencing *PTGS2* in Skov3-ip1 cells *in vivo* completely abrogated stress-mediated changes in tumor growth and metastasis.

The role of adrenergic signaling mediating inflammation and metastasis has been studied in other cell types within the tumor microenvironment. Studies in breast cancer have shown that enhanced macrophage recruitment into the primary site increases the rate of metastasis and that this process is mediated by adrenergic receptors¹⁵. Shakhar and Ben-Eliyahu showed that activation of the SNS can suppress natural killer cell activity *in vivo*¹⁶. The same group also showed that the combination of beta-blockers and Cox2 inhibitors can enhance immune response by reversing surgery-induced decreases in NK cell activity¹⁷. Other studies have shown that tumor cells can produce interleukin-6, interleukin-8, and other pro-inflammatory molecules *via* adrenergic signaling^{1,18}.

Our studies have shown that 59% of ovarian cancer patients present in the clinic with depressed mood commensurate with clinical depression (CESD greater than or equal to 16) and transcriptome analysis in these patients showed elevated CREB and Nf-kB signaling^{1,4,19}. Because Nf-kB has been shown to be a link between several cancer cell signaling pathways and inflammation, we focused on Nf-kB as the main transcription factor that mediates stress-induced modifications of PGE2 production²⁰. PGE2 is a key biolipid metabolite that is commonly associated with increased metastasis, angiogenesis, and cell proliferation and decreased apoptosis, but the most potent function of PGE2 is to increase

chronic inflammation within tumors²¹. It does so by potently recruiting neutrophils and macrophages and shifting the T-cell population toward T-helper 17 pro-inflammatory cells within the tumor microenvironment²¹⁻²³. High combined expression levels of *ADRB2*, *PTGS2* and *PTGES* were associated with decreased overall and progression-free survival in patients with high-grade serous ovarian cancer in TCGA datasets. In ovarian cancer, PGE2 synthesis and elevated *PTGS2* is associated with malignant transformation^{24,26}. *PTGS2* in ovarian cancer is associated with reduced survival rates^{27,28}. Studies using Skov3 and OVCAR5 cells have shown that EGF-driven PGE2 synthesis can drive cancer cell invasion *in vitro* that is consistent with data presented in the current study²⁵.

The key findings from our study are that adrenergic pathways can directly influence inflammation-related pathways by increasing pro-inflammatory prostaglandins that can contribute significantly to tumor metastasis. Adrenergic receptors and *PTGS2* are viable pharmaceutical targets; several of these are approved by the US Food and Drug Administration for treatment of various human diseases. The current study has immense translational potential, providing a rationale for combining a beta-blocker such as propranolol with celecoxib or aspirin to block both inflammation and metastasis.

Methods

Cell lines and treatment

Skov3-ip1 and HeyA8 ovarian cancer cells were maintained in RPMI-1640 media supplemented with 15% fetal bovine serum and 0.1% gentamycin sulfate at 37°C in a humidified incubator. Cells at 70% confluence were serum-starved overnight for treatment with NE, agonists, or antagonists. NE (10µM; Sigma Aldrich, St. Louis, MO) was dissolved in sterile water just before it was added to the cells. Isoproterenol, dobutamine, and terbutaline were purchased from Sigma and used at previously published concentrations⁶. CL316243, propranolol, atenolol butoxamine were purchased from Tocris (Bristol, UK) and used at previously published concentrations⁶. Cells were treated with antagonists for 1 hour before NE was added to the cell culture media. *PTGS2* was silenced using reverse transfection protocol with RNAimax and specific human-*PTGS2* siRNA (sequence: GAGTATGCGATGTGCTTAA; Sigma Aldrich (St. Louis, MO)) according to manufacturer recommendations. Briefly, 40nM siRNA was mixed with RNAimax transfecting agent and added to culture media for 4 hours. Fresh media was added and cells were allowed to grow. Silencing was assessed at 48 hours using qRT-PCR analysis.

Restraint stress model

The Institutional Animal Care and Use Committee at The University of Texas MD Anderson Cancer Center approved all animal experiments. All animal experiments were performed in 8- to 12-week-old female athymic nude mice obtained from Taconic Farms (Hudson, NY). We used a previously described and well-defined restraint stress procedure to induce symptoms of stress experimentally⁶. In this model, mice are securely restrained in a movement-restricted space for 2 hours daily during the duration of the experiment. In all experiments, 1×10^6 Skov3-ip1 or 0.25×10^5 HeyA8 ovarian cancer cells were injected either intraperitoneally or into the ovaries (to study metastasis) in mice 1 week after the

restraint stress procedure began. Ten mice were assigned to each group, and 5 days after cancer cell injection, treatment with siRNA was started (control or human *PTGS2* siRNA, biweekly, 3.5 µg siRNA in DOPC nanoparticles per injection). For blocker experiments, the animals were treated daily with propranolol or butoxamine as previously reported⁶. After 28 days, the animals were killed by cervical dislocation, and tumor weight, number of tumor nodules, and distribution of metastases were noted by researchers blinded to the groups.

Patient samples

Tumor samples from ovarian cancer patients were obtained as previously described⁴. Briefly, 55 patients took bibehavioral assessments prior to surgery. Depressive symptoms were assessed using the CES-D scale and a score >16 were considered to indicate high levels of depression. Based on the results, 33 patients had a low-depression score and 22 patients had a high-depression score. A pathologist also analyzed tumors for stage, grade, and histologic subtype. Fifteen normal ovarian tissue controls (post-menopausal) were also obtained. Institutional Review Boards at the University of Iowa and MD Anderson approved all procedures and consent of patients was obtained.

Metabolic profiling

All metabolite analysis was performed at Metabolon Inc. (Durham, NC). Patient and orthotopic tumor samples were snap frozen and shipped to Metabolon. Briefly, methanol extraction of small molecules was carried out as described previously^{29,30} using 100 µL of homogenate per sample. Ultra-high performance liquid chromatography–tandem mass spectrometry and gas chromatography–mass spectrometry were used to assess absolute quantities of >200 metabolites in each sample. Identification of known chemical entities was based on comparison to metabolomic library entries of more than 4,000 purified standards.

Immunoblotting

Cell and tumor protein lysates were prepared in RIPA buffer supplemented with protease and phosphatase inhibitors. Equal quantities of protein lysates were resolved on a denaturing SDS-PAGE gel and transferred to a nitrocellulose membrane. After blocking the membrane in 5% milk in TBS-T for an hour at room temperature, we incubated the membrane with primary antibodies (PTGS2: catalog #160112, 1:1000 in 5% milk in TBS-T; Cayman Chemicals (Ann Harbor, MI),) overnight at 4°C. Blots were washed and incubated with HRP-conjugated secondary antibody (GE Health Sciences, Pittsburgh, PA)) for an hour and developed using a chemiluminescent detection system (GE Health Sciences). Loading control beta-actin (A5316; Sigma Aldrich (St. Louis, MO)) was probed similarly after the blot was stripped using Restore Stripping Buffer (Pierce, Rockford, IL)

Immunostaining

Paraffin-embedded slides were deparaffinized, dehydrated, and rehydrated using a series of acetone and alcohol washes. Antigen retrieval was performed using citrate buffer at pH 6.0 in a pressure cooker. The primary antibody (PTGS2: 160112, 1:100; Cayman Chemicals) was prepared in 4% fish gelatin and incubated with the slides overnight at 4°C. Slides were then washed and incubated with HRP-conjugated secondary antibody (Jackson Immuno

Research, West Grove, PA) at room temperature for 1 hour. DAB substrate (Invitrogen, Grand Island, NY) was used to visualize staining of protein and hematoxylin (Invitrogen) was used to stain nuclei. For immunocytochemistry experiments, Skov3-ip1 and HeyA8 cells were grown in chamber slides prior to treatment with NE. Cells were fixed in 4% paraformaldehyde and permeabilized using Triton X-100. Staining using primary (PTGES: 1:100; T6079, Sigma Aldrich, p-Nf- κ B: 1:100; 3033S, Cell Signaling, total Nf- κ B: 1:100, 8242S, Cell Signaling) and secondary antibodies (anti-rabbit Alexa Flour 594, 1:800; Jackson Immuno Research) was done as described above. Hoechst (Invitrogen) was used to stain nuclei.

ChIP analysis

Skov3-ip1 cells were used to study binding of Nf- κ B to PTGS2 and PTGES promoter after treatment with NE. Briefly, cells were serum starved overnight and treated with NE for 2 hours. For ChIP analysis, the cells were collected and samples prepared according to the ChIP-IT express protocol (Active Motif, Carlsbad, CA) and ChIP-grade Nf- κ B antibody (8242S, Cell Signal, Boston, MA) was used to pull down the genomic sequence bound to Nf- κ B. qRT-PCR was used to quantify the relative enrichment of the promoter region after treatment with NE. The primer sequences used were as follows: PTGS2: forward: AAAGACGTACAGACCAGACACG, reverse: AGAAGGACACTTGGCTTCCTC; PTGES: forward: TTTTACTGCCTCCCTCTTGG, reverse: AACCCGTGACTGTGACTATGTG. For Nf- κ B transcription factor assay, cells were prepared similar to ChIP and assessed using NF- κ B (human p50/p65) Combo Transcription Factor Assay Kit (10011223, Cayman Chemicals) according to manufacturer instructions.

Invasion and migration

Skov3-ip1 cells were used to study migration and invasion *in vitro*. Inserts (8 μ M; Millipore, Billerica, MA) were coated with 1% gelatin for migration and gelatin-fibronectin for invasion assays. A total of 50,000 cells were placed in upper wells and allowed to move toward conditioned media in the presence or absence of NE and with control or PTGS2 siRNA. Migration was assessed at 6 hours and invasion at 24 hours of treatment with NE by fixing the cells in Protocol Hema3 (Thermo Fisher Scientific, Waltham, MA). Cells were counted in random high-power fields, and cell counts were reported as average cells migrated or invaded.

qRT-PCR

Total RNA was extracted from cells using the Zymo Research RNA isolation kit with TRIzol reagent (Invitrogen), according to standard manufacturer protocols. Complementary DNA was synthesized from 1 μ g of total RNA using the Verso cDNA synthesis kit (Thermo Scientific, Pittsburgh, PA) according to the supplier protocol, using random hexamers and oligo-dT primers in a 3:1 ratio. Quantitative PCR was performed using SYBR green master mix on the 7500 Real-Time PCR System (Applied Biosystems, Carlsbad, CA) using standard protocols. The primer sequences used are as follows: PTGS2: forward: CCCTTGGGTGTCAAAGGTAA, reverse: GCCCTCGCTTATGATCTGTC; PTGES: forward: GGAAGACCAGGAAGTGCATC, reverse: AGTATTGCAGGAGCGACCC.

ELISA

ELISA analysis for PGE2 levels was performed using the PGE2 ELISA kit from Cayman Chemicals according to manufacturer recommendations. Skov3-ip1 and HeyA8 cells were grown to 70% confluence and serum-starved overnight. Fresh serum-free media was added with 10 μ M NE and specific antagonists or agonists were added as described above. Cell culture media was collected 24 hours later and stored at -80°C until analysis.

Statistical analyses

Microsoft Excel or GraphPad Prism (Microsoft, Redmond, WA) was used to analyze data. Continuous variables were compared using the Student *t* test or analysis of variance, and the Mann-Whitney test was used to compare differences. Using 2-way analysis of variance, we determined that a sample size of 10 animals per group would provide an effective size of 1.3 with 80% power at a significance level of $p = 0.05$. We considered $p < 0.05$ to be statistically significant. For the metabolic analysis, Welch 2-sample *t* tests were used to identify biochemicals that differed significantly ($p < 0.05$) between experimental groups using Array Studio software (OmicSoft). All statistical analyses were expressed as mean \pm standard error of the mean.

Supplementary Material

Refer to Web version on PubMed Central for supplementary material.

Acknowledgments

We thank the following for funding support: United States National Institutes of Health (CA116778, CA104825, CA140933, CA109298, CPRIT RP140106, NIH CA 109298, P50CA083639, P50CA098258, AG017265, AG033590) and the Breast Cancer Research Foundation, the United States Department of Defense (OC073399, W81XWH-10-1-0158, and BC085265); the Marcus Foundation; the Red and Charline McCombs Institute for the Early Detection and Treatment of Cancer; the RGK Foundation; the Gilder Foundation; the Blanton-Davis Ovarian Cancer Research Program; and the Betty Anne Asche Murray Distinguished Professorship (A.K.S.).

A.N. is supported in part by the CPRIT Graduate Scholar Fellowship. K.M.G. is supported Altman-Goldstein Discovery fellowship. S.Y.W. is supported by the Ovarian Cancer Research Fund, Inc., and by Cancer Prevention and Research Institute of Texas training grants (RP101502 and RP101489). R.A.P., B.Z., and J.H. are supported by the NCI-DHHS-NIH T32 training grant (T32 CA101642).

We would like to thank Laila Dahmouh at University of Iowa for her help analyzing patient tumor slides. We would also like to thank Erica Goodoff at MD Anderson for help with scientific editing.

References

1. Costanzo ES, et al. Psychosocial factors and interleukin-6 among women with advanced ovarian cancer. *Cancer*. 2005; 104:305–313. DOI: 10.1002/Cncr.21147 [PubMed: 15954082]
2. Hassan S, et al. Behavioral stress accelerates prostate cancer development in mice. *The Journal of clinical investigation*. 2013; 123:874–886. DOI: 10.1172/JCI63324 [PubMed: 23348742]
3. Kruk J, Aboul-Enein HY. Psychological stress and the risk of breast cancer: a case-control study. *Cancer detection and prevention*. 2004; 28:399–408. DOI: 10.1016/j.cdp.2004.07.009 [PubMed: 15582263]
4. Lutgendorf SK, et al. Depression, social support, and beta-adrenergic transcription control in human ovarian cancer. *Brain, behavior, and immunity*. 2009; 23:176–183. DOI: 10.1016/j.bbi.2008.04.155
5. Ramirez AJ, et al. Stress and relapse of breast cancer. *Bmj*. 1989; 298:291–293. [PubMed: 2493899]

6. Thaker PH, et al. Chronic stress promotes tumor growth and angiogenesis in a mouse model of ovarian carcinoma. *Nature medicine*. 2006; 12:939–944. DOI: 10.1038/nm1447
7. Lutgendorf SK, et al. Social influences on clinical outcomes of patients with ovarian cancer. *Journal of clinical oncology : official journal of the American Society of Clinical Oncology*. 2012; 30:2885–2890. DOI: 10.1200/JCO.2011.39.4411 [PubMed: 22802321]
8. Wang HM, et al. Improved survival outcomes with the incidental use of beta-blockers among patients with non-small-cell lung cancer treated with definitive radiation therapy. *Annals of Oncology*. 2013; 24:1312–1319. DOI: 10.1093/annonc/mds616 [PubMed: 23300016]
9. Sood AK, et al. Stress hormone-mediated invasion of ovarian cancer cells. *Clinical cancer research : an official journal of the American Association for Cancer Research*. 2006; 12:369–375. DOI: 10.1158/1078-0432.CCR-05-1698 [PubMed: 16428474]
10. Sethi J, et al. Antioxidant effect of *Triticum aestivum* (wheat grass) in high-fat diet-induced oxidative stress in rabbits. *Methods and findings in experimental and clinical pharmacology*. 2010; 32:233–235. DOI: 10.1358/mf.2010.32.4.1423889 [PubMed: 20508870]
11. Gosain A, Jones SB, Shankar R, Gamelli RL, DiPietro LA. Norepinephrine modulates the inflammatory and proliferative phases of wound healing. *J Trauma*. 2006; 60:736–743. DOI: 10.1097/01.ta.0000196802.91829.cc [PubMed: 16612292]
12. Sivamani RK, et al. Stress-Mediated Increases in Systemic and Local Epinephrine Impair Skin Wound Healing: Potential New Indication for Beta Blockers. *Plos Med*. 2009; 6:105–115. ARTN e1000012. DOI: 10.1371/journal.pmed.1000012
13. Radloff LS. The CES-D Scale: A Self-Report Depression Scale for Research in the General Population. *Applied Psychological Measurement*. 1977; 1:385–401. DOI: 10.1177/014662167700100306
14. Kosaka T, et al. Characterization of the human gene (PTGS2) encoding prostaglandin-endoperoxide synthase 2. *European journal of biochemistry/FEBS*. 1994; 221:889–897. [PubMed: 8181472]
15. Sloan EK, et al. The sympathetic nervous system induces a metastatic switch in primary breast cancer. *Cancer research*. 2010; 70:7042–7052. DOI: 10.1158/0008-5472.CAN-10-0522 [PubMed: 20823155]
16. Shakhar G, Ben-Eliyahu S. In vivo beta-adrenergic stimulation suppresses natural killer activity and compromises resistance to tumor metastasis in rats. *J Immunol*. 1998; 160:3251–3258. [PubMed: 9531281]
17. Benish M, et al. Perioperative use of beta-blockers and COX-2 inhibitors may improve immune competence and reduce the risk of tumor metastasis. *Ann Surg Oncol*. 2008; 15:2042–2052. DOI: 10.1245/s10434-008-9890-5 [PubMed: 18398660]
18. Yang EV, et al. Norepinephrine upregulates VEGF, IL-8, and IL-6 expression in human melanoma tumor cell lines: implications for stress-related enhancement of tumor progression. *Brain, behavior, and immunity*. 2009; 23:267–275. DOI: 10.1016/j.bbi.2008.10.005
19. Lutgendorf SK, et al. Social isolation is associated with elevated tumor norepinephrine in ovarian carcinoma patients. *Brain, behavior, and immunity*. 2011; 25:250–255. DOI: 10.1016/j.bbi.2010.10.012
20. Bierhaus A, et al. A mechanism converting psychosocial stress into mononuclear cell activation. *Proceedings of the National Academy of Sciences of the United States of America*. 2003; 100:1920–1925. DOI: 10.1073/pnas.0438019100 [PubMed: 12578963]
21. Wang D, Dubois RN. Eicosanoids and cancer. *Nature reviews. Cancer*. 2010; 10:181–193. DOI: 10.1038/nrc2809 [PubMed: 20168319]
22. Kalinski P. Regulation of immune responses by prostaglandin E2. *Journal of immunology*. 2012; 188:21–28. DOI: 10.4049/jimmunol.1101029
23. Greenhough A, et al. The COX-2/PGE2 pathway: key roles in the hallmarks of cancer and adaptation to the tumour microenvironment. *Carcinogenesis*. 2009; 30:377–386. DOI: 10.1093/carcin/bgp014 [PubMed: 19136477]
24. Lin Y, Cui M, Xu T, Yu W, Zhang L. Silencing of cyclooxygenase-2 inhibits the growth, invasion and migration of ovarian cancer cells. *Molecular medicine reports*. 2014; 9:2499–2504. DOI: 10.3892/mmr.2014.2131 [PubMed: 24718658]

25. Qiu X, Cheng JC, Chang HM, Leung PC. COX2 and PGE2 mediate EGF-induced E-cadherin-independent human ovarian cancer cell invasion. *Endocrine-related cancer*. 2014; 21:533–543. DOI: 10.1530/ERC-13-0450 [PubMed: 24969217]
26. Matsumoto Y, Ishiko O, Deguchi M, Nakagawa E, Ogita S. Cyclooxygenase-2 expression in normal ovaries and epithelial ovarian neoplasms. *International journal of molecular medicine*. 2001; 8:31–36. [PubMed: 11408945]
27. Athanassiadou P, et al. The prognostic significance of COX-2 and survivin expression in ovarian cancer. *Pathology, research and practice*. 2008; 204:241–249. DOI: 10.1016/j.prp.2007.11.004
28. Denkert C, et al. Expression of cyclooxygenase 2 is an independent prognostic factor in human ovarian carcinoma. *Am J Pathol*. 2002; 160:893–903. DOI: 10.1016/S0002-9440(10)64912-7 [PubMed: 11891188]
29. Evans AM, DeHaven CD, Barrett T, Mitchell M, Milgram E. Integrated, nontargeted ultrahigh performance liquid chromatography/electrospray ionization tandem mass spectrometry platform for the identification and relative quantification of the small-molecule complement of biological systems. *Analytical chemistry*. 2009; 81:6656–6667. DOI: 10.1021/ac901536h [PubMed: 19624122]
30. Weiner J 3rd, et al. Biomarkers of inflammation, immunosuppression and stress with active disease are revealed by metabolomic profiling of tuberculosis patients. *PloS one*. 2012; 7:e40221. [PubMed: 22844400]

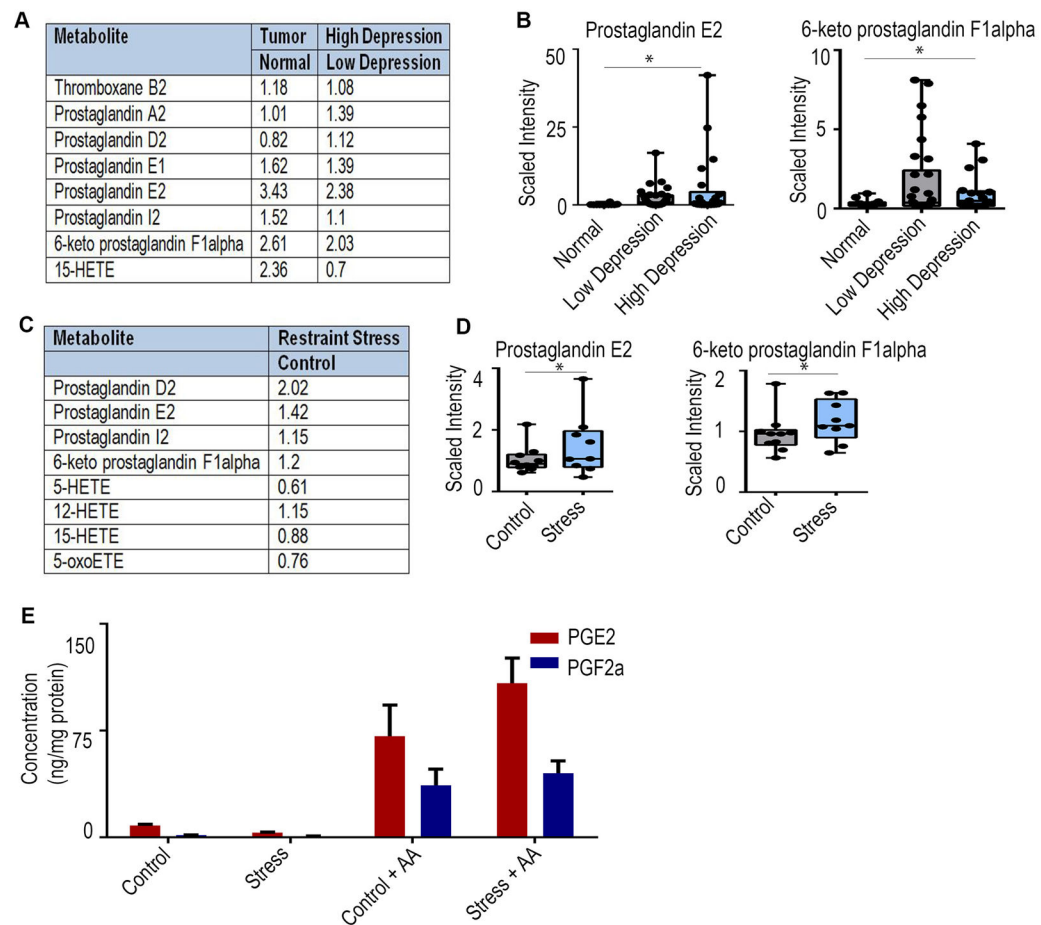


Figure 1. Chronic stress increases levels of prostaglandins

A, Primary ovarian tumors were obtained from clinical samples and analyzed for global metabolite levels. Fold changes in eicosanoids are shown in clinical samples from those with high levels of depression relative to those with low levels of depression (based on standardized assessment scores), as well as in tumor samples relative to normal ovarian tissue samples. B, Levels of prostaglandin E2 and 6-keto prostaglandin F1 alpha in clinical tumor samples from patients with no tumor (normal ovarian tissue), patients with low depression scores, and patients with high depression scores. C, Female athymic nude mice were injected with Skov3-ip1 cells and randomized to control or daily restraint groups. Mice were stressed for a week and tumors were harvested after the mice were euthanized. Shown here are fold changes in levels of eicosanoids in tumors obtained from mice subjected to daily restraint stress relative to control mice. E, Levels of prostaglandin E2 and 6-keto prostaglandin F1 alpha in orthotopic tumors from control mice and mice subjected to daily restraint stress. F, Tumors obtained from control mice and mice subjected to daily restraint stress were incubated with exogenous arachidonic acid (AA) and prostaglandin E2 (PGE2) or 6-keto prostaglandin F1 alpha (PGF2a) and analyzed using mass spectrometry.

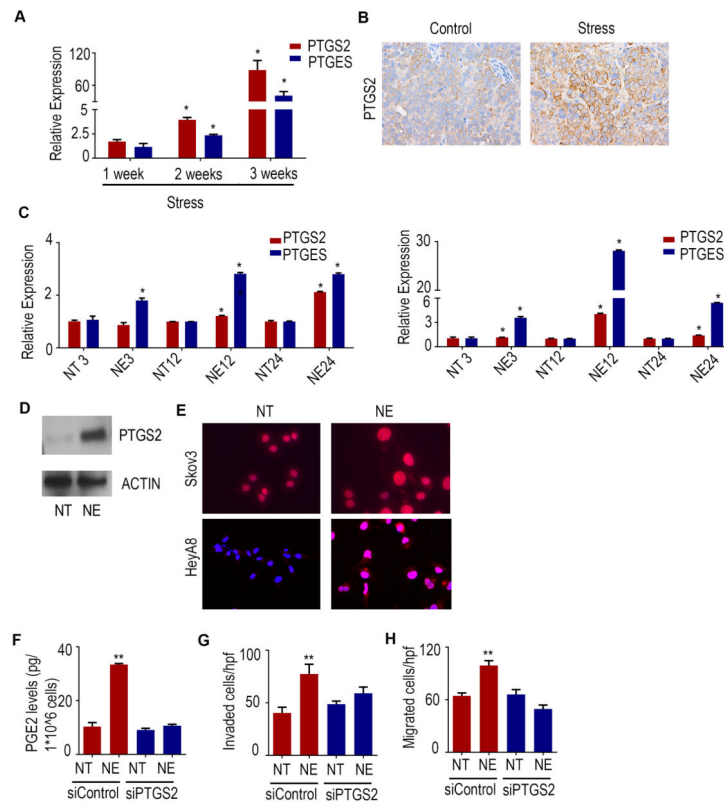


Figure 2. Adrenergic signaling increases levels of PTGS2 and PTGES

A, Mice bearing Skov3-ip1 tumors underwent daily restraint stress for 1, 2, or 3 weeks. Mice were euthanized and tumors were analyzed for expression of PTGS2 and PTGES using human-specific primers. B, Expression of PTGS2 in representative images of orthotopic tumors from control and stressed mice in an Skov3-ip1 model (magnification at 20X). C, Relative expression of PTGS2 and PTGES after treatment of Skov3-ip1 and HeyA8 cells with 10 μ M norepinephrine (NE) at various time points (numbers indicate hours; data are normalized to non-treated [NT] cells). D, Representative Western blot images showing protein expression of PTGS2 in Skov3-ip1 and HeyA8 cells after treatment with NE for 24 hours. Actin was used as a loading control. E, Representative immunocytochemical images showing protein expression of PTGES in Skov3-ip1 and HeyA8 cells after treatment with NE for 24 hours. F, Skov3-ip1 cells were transfected with control or PTGS2 siRNA before treatment with NE. Levels of PGE2 in culture media was assessed by ELISA. G, *In vitro* invasive potential through a defined basement membrane matrix for 24 hours was assessed by fixing and counting the number of cells invaded per high-power field (hpf). H, *In vitro* migratory potential through 0.1% gelatin over 6 hours was assessed by fixing and counting the number of cells migrated per hpf. In all experiments, n = 3 per group and data are presented as mean \pm standard error of the mean (error bars). Statistical significance was obtained using the Student *t* test: **p* < 0.05, ***p* < 0.01 (compared with NT or siControl cells).

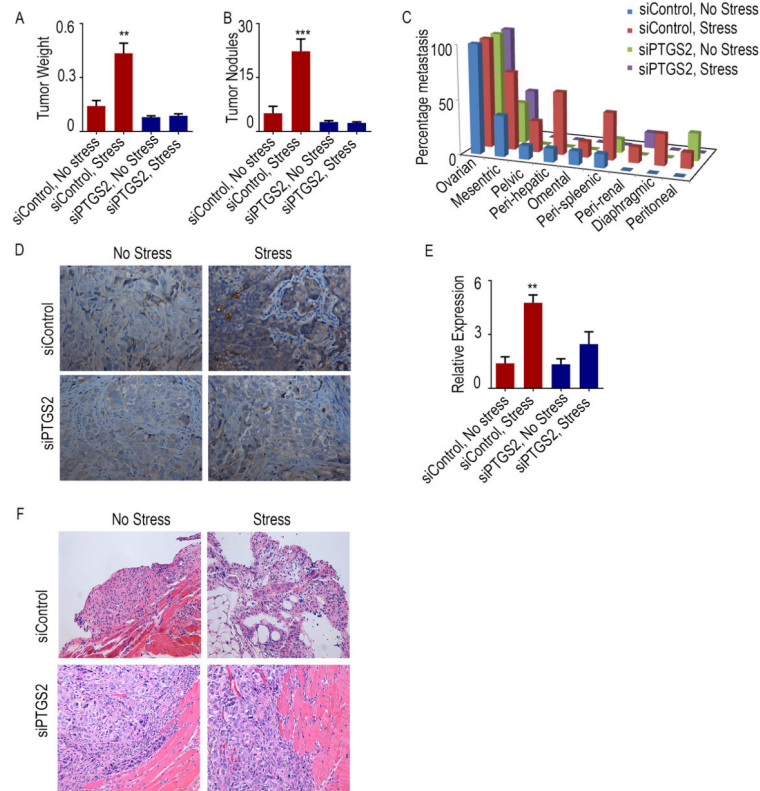


Figure 3. Effect of silencing PTGS2 *in vivo*

A and B, Female athymic nude mice were injected with Skov3-ip1 cells and subjected to daily restraint stress (or control) and then treated twice per week with either control siRNA or PTGS2 siRNA. Mice were euthanized and tumor weight and the number of nodules were noted. C, Frequency of metastasis in mice subjected to daily restraint stress (or control) and treated with control or PTGS2 siRNA. D, Validation of siRNA efficiency in immunohistochemical stains showing tumor cell-specific knockdown of PTGS2 (magnification of 20x) E, siRNA efficiency was also validated using quantitative reverse-transcription polymerase chain reaction with human-specific primers. 18S was used as a control gene. F, Representative images showing hematoxylin and eosin staining for each group in the Skov3-ip1 ovarian cancer mouse model (magnification of 20x). In all experiments, $n = 10$ for each group and data are presented as mean \pm standard error of the mean. Statistical significance was obtained using the Student t test: * $p < 0.05$, ** $p < 0.01$, *** $p < 0.001$.

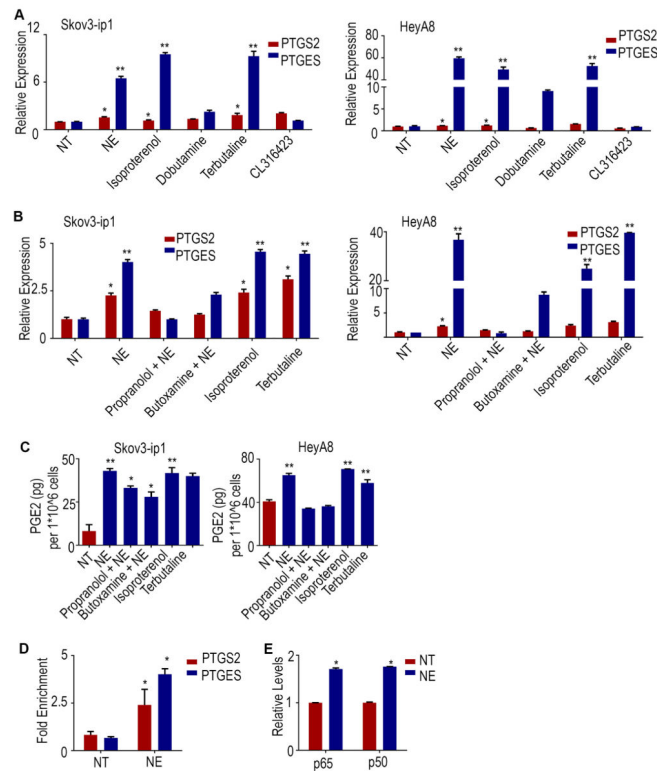


Figure 4. Mechanism of PTGS2 induction downstream of norepinephrine (NE)

A, Skov3-ip1 (left) and HeyA8 (right) cells were treated with NE, isoproterenol (a broad ADRB agonist), and specific beta-agonists (ADRB1: dobutamine; ADRB2: terbutaline; ADRB3: CL316423) and assessed for expression of PTGS2 and PTGES. B, Skov3-ip1 (left) and HeyA8 (right) cells were treated with propranolol (broad ADRB antagonist) and butoxamine (ADRB2-specific antagonist) prior to treatment with NE. Isoproterenol and terbutaline were included as positive controls. C, Enzyme-linked immunosorbent assay results showing PGE2 levels in conditioned media from Skov3-ip1 (left) and HeyA8 (right) cells treated with NE, isoproterenol, terbutaline, propranolol plus NE, and butoxamine plus NE. D, Chromatin was obtained from Skov3-ip1 cells treated with NE and incubated with specific Nf-kB antibodies. Quantitative reverse-transcription polymerase chain reaction was then used to assess fold enrichment of Nf-kB on the promoters of PTGS2 and PTGES, normalized to non-treated (NT) cells. E, Nuclear proteins were isolated from Skov3-ip1 cells treated with NE and levels of p65 and p50 in the nucleus were compared with levels in NT cells, assessed as fold changes. In all experiments, $n = 3$ per group and data are presented as mean \pm standard error of the mean. Statistical significance was obtained using the Student t test: * $p < 0.05$, ** $p < 0.01$ (compared with NT cells).

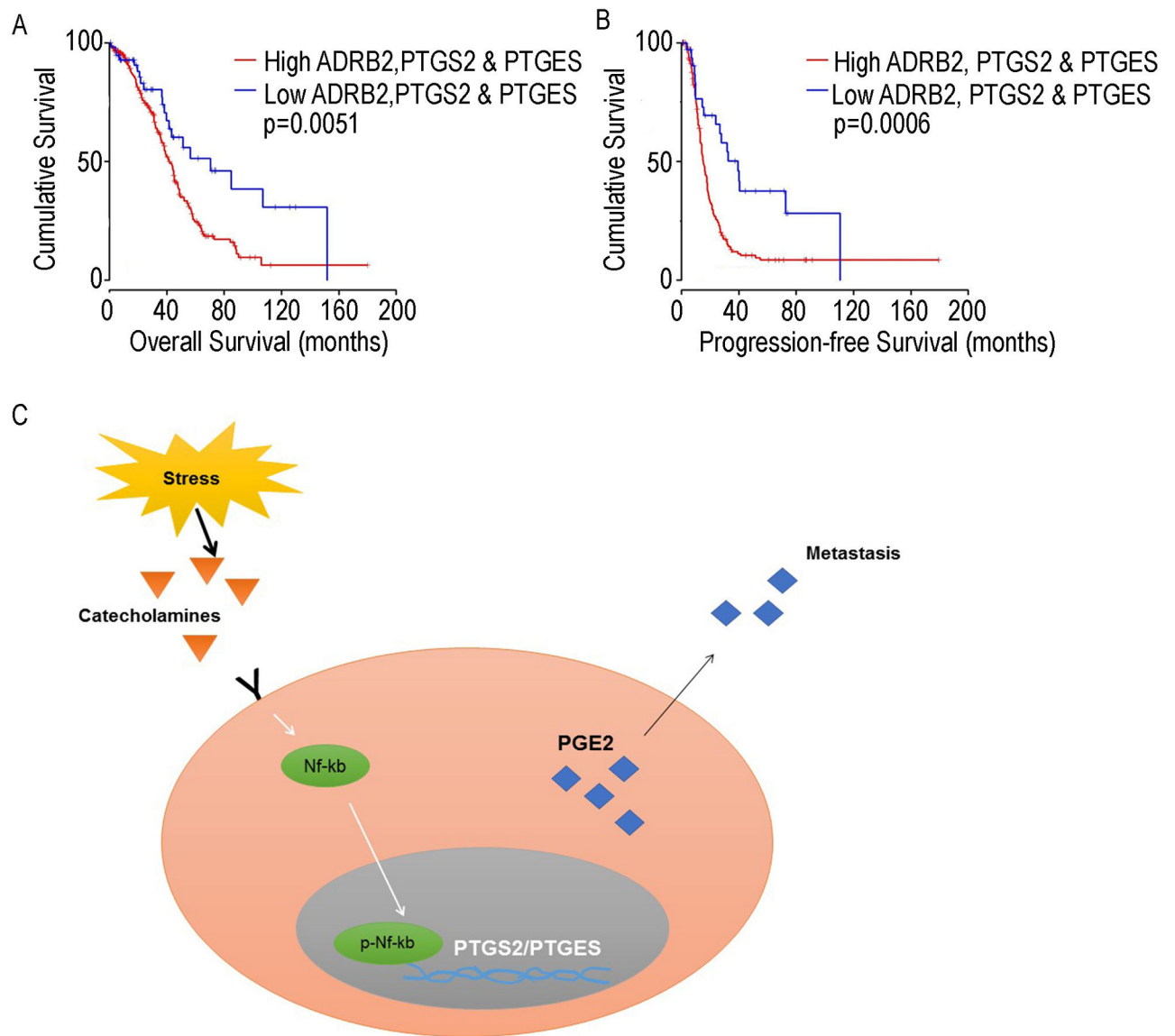


Figure 5. Clinical relevance of PTGS2 and PTGES in ovarian cancer

A and B, Kaplan-Meier plots for overall survival and progression-free survival in patients with ovarian cancer, based on combined expression of PTGS2 and PTGES. Data were pulled from The Cancer Genome Atlas project. C, A model for PGE2 synthesis during sustained adrenergic signaling and the role of PGE2 in metastasis.